

# Phenyl-Conjugated Oligoene Sensitizers for TiO<sub>2</sub> Solar Cells

Takayuki Kitamura,<sup>†,‡</sup> Masaaki Ikeda,<sup>§</sup> Koichiro Shigaki,<sup>§</sup> Teruhisa Inoue,<sup>§</sup>  
Neil A. Anderson,<sup>‡</sup> Xin Ai,<sup>‡</sup> Tianquan Lian,<sup>‡</sup> and Shozo Yanagida<sup>\*,†</sup>

Material and Life Science, Graduate School of Engineering, Osaka University,  
Suita, Osaka 565-0871, Japan, Department of Chemistry, Emory University,  
Atlanta, Georgia 30322, and Functional Chemicals Research Laboratories,  
Nippon Kayaku Co., Ltd., Kita-ku, Tokyo 115-0042, Japan

Received October 7, 2003. Revised Manuscript Received February 5, 2004

As highly efficient organic sensitizers for dye-sensitized solar cells, a series of novel oligoene dyes which have different lengths of methine units, cyano groups and/or carboxylic groups as the electron acceptor units, and amino groups as the electron donor units was designed and synthesized. The bathochromic shift of the absorption spectrum was achieved by expansion of the  $\pi$ -conjugated system by increasing the number of methine units and by introduction of both electron-withdrawing and -accepting groups, which induced charge-transfer-type absorption character. Redox potential of the dyes was also controlled by the substitution of the functional groups. Dye-sensitized solar cells (DSCs) based on the oligoene dyes showed excellent response of incident photon to current conversion efficiency (>80%), leading to good photovoltaic performances up to 6.6% under 1 sun irradiation conditions. Femtosecond transient absorption spectroscopy in the mid-IR region revealed the very fast electron injection from the excited states of the oligoene dyes to the conduction band of TiO<sub>2</sub>. The molecular design of oligoene dye is reliable for developing novel organic sensitizers for use in dye-sensitized solar cells.

## Introduction

The dye-sensitized solar cell (DSC) is currently under intense investigation for its respectable photoconversion efficiency up to 10%, low materials and production costs, and the viewpoints of life cycle assessment in mass production.<sup>1,2</sup> With regard to the sensitizer (dye), several ruthenium polypyridine complexes, such as *cis*-dithiocyanato bis(4,4'-dicarboxy-2,2'-bipyridine)ruthenium(II) (so-called N3),<sup>1,2</sup> its bis(tetrabutylammonium) salt (N719),<sup>3</sup> and trithiocyanato (4,4',4''-tricarboxy-2,2':6',2''-terpyridine)ruthenium(II) (black dye),<sup>4,5</sup> gave the best photoconversion efficiencies of the examined dyes for DSC thus far. Ruthenium complexes have many advantageous features for application as sensitizers for DSCs.<sup>6</sup>

First, such complexes have broad metal-to-ligand charge-transfer (MLCT) absorption bands, covering a wide spectral range from near UV to visible. Second, the photoexcited states and oxidized form of the complexes are chemically stable and have appropriate redox potentials for electron injection to TiO<sub>2</sub> and for accepting electrons from the I<sup>-</sup>/I<sub>3</sub><sup>-</sup> redox couple in the electrolyte. For the mass production of DSC in practical applications, however, development of alternative synthetic organic dyes is required because the ruthenium dyes are quite expensive and the limited resources of ruthenium will be a critical issue.

While organic dyes such as xanthene dyes were employed in earlier studies of dye sensitization of semiconductors,<sup>7,8</sup> little attention had been paid to the use of organic dyes for DSC in the past decade. Perylenes,<sup>9,10</sup> 9-phenylxanthenes,<sup>11</sup> triphenylmethanes,<sup>12</sup> and some natural dyes<sup>13,14</sup> were applied for the sensitizer, but DSCs based on such organic dyes showed poor

\* To whom correspondence should be addressed. Phone: +81-6-6879-7924. Fax: +81-6-6879-7875. E-mail: yanagida@mls.eng.osaka-u.ac.jp.

<sup>†</sup> Osaka University

<sup>‡</sup> Emory University

<sup>§</sup> Nippon Kayaku Co.

(1) O'Regan, B.; Grätzel, M. *Nature* **1991**, *353*, 737.

(2) Nazeeruddin, M. K.; Kay, A.; Rodicio, I.; Humphry-Baker, R.; Müller, E.; Liska, P.; Vlachopoulos, N.; Grätzel, M. *J. Am. Chem. Soc.* **1993**, *115*, 6382.

(3) Nazeeruddin, M. K.; Zakeeruddin, S. M.; Humphry-Baker, R.; Jirousek, M.; Liska, P.; Vlachopoulos, N.; Shklover, V.; Fischer, C.-H.; Grätzel, M. *Inorg. Chem.* **1999**, *38*, 6298.

(4) Nazeeruddin, M. K.; Péchy, P.; Grätzel, M. *Chem. Commun.* **1997**, 1705.

(5) Nazeeruddin, M. K.; Péchy, P.; Renouard, T.; Zakeeruddin, S. M.; Humphry-Baker, R.; Comte, P.; Liska, P.; Cevey, L.; Costa, E.; Shklover, V.; Spiccia, L.; Deacon, G. B.; Bignozzi, C. A.; Grätzel, M. *J. Am. Chem. Soc.* **2001**, *123*, 1613.

(6) Kalayansundaram, K.; Grätzel, M. *Coord. Chem. Rev.* **1998**, *77*, 347.

(7) Gerischer, H.; Tributsch, H. *Ber. Bunsen-Ges. Phys. Chem.* **1968**, *72*, 437.

(8) Tsubomura, H.; Matsumura, M.; Nomura, Y.; Amamiya, T. *Nature* **1976**, *261*, 402.

(9) Ferrere, S.; Zaban, A.; Gregg, B. A. *J. Phys. Chem. B* **1997**, *101*, 4490.

(10) Ferrere, S.; Gregg, B. A. *New J. Chem.* **2002**, *26*, 1155.

(11) Sayama, K.; Sugino, M.; Sugihara, H.; Arakawa, H. *Chem. Lett.* **1998**, 753.

(12) Jayaweera, P. M.; Kumarasinghe, A. R.; Tennakone, K. *J. Photochem. Photobiol. A: Chem.* **1998**, *126*, 111.

(13) Cherepy, N. J.; Smestad, G. P.; Grätzel, M.; Zhang, J. Z. *J. Phys. Chem. B* **1997**, *101*, 9342.

(14) Tennakone, K.; Kumara, G. R. R. A.; Kottegoda, I. R. M.; Perera, V. P. S.; Weerasundara, P. S. R. S. *J. Photochem. Photobiol. A: Chem.* **1998**, *117*, 137.

conversion efficiencies. More recently, significantly improved performances of DSCs with organic dyes were reported from Arakawa's group. Some benzothiazole merocyanines formed J-aggregates on the surface of TiO<sub>2</sub>, which have absorption extending to 680 nm.<sup>15,16</sup> A merocyanine dye with a long alkyl chain that forms tight aggregates on the TiO<sub>2</sub> surface shows 4.2% conversion efficiency under 1 sun irradiation conditions.<sup>16</sup> Some coumarin dyes were also applied as sensitizers of DSC, and a sterically hindered coumarin dye gave a 5.6% conversion efficiency with 80% incident photon-to-current conversion efficiency (IPCE) at 470 nm.<sup>17–19</sup> Coumarin dyes with oligothiophene units show extremely high conversion efficiencies, and up to 7.7% conversion efficiency has been achieved.<sup>20</sup> Spitlar also studied some cyanine dyes with two carboxylic acid groups<sup>21,22</sup> and discussed the effects of the "spacer" between the chromophore and anchoring carboxylic group on aggregation of dye on the TiO<sub>2</sub> surface, on the absorption spectrum, and on the short circuit photocurrent density and action spectra of photocurrent. They succeeded in the expansion of spectral response of the cell by using multiple dyes on one electrode and observed 8.4 mA·cm<sup>-2</sup> of photocurrent density for a 4- $\mu$ m-thick electrode as the maximum value under Xe lamp illumination.<sup>22</sup> Huang and co-workers examined hemicyanine derivatives as a sensitizer for DSC and introduced alkylsulfonic acid<sup>23–26</sup> or multiple carboxylic acids<sup>27,28</sup> as the anchoring group. While they used a light source different from AM 1.5 standard and the reported IPCE values were too high to be reliable with taking into account the reflection and absorption of glass substrate, it is credible that most of the hemicyanine dyes examined could work as good sensitizers for DSC.

At the moment, the requirements of efficient sensitizing dyes for use in DSC are stated as follows:<sup>6,16,25</sup> (1) Wide absorption band (panchromatic) and high absorption coefficient that give high light harvesting efficiency to provide large photocurrent; (2) appropriate redox potentials of the LUMO level for electron injection to the conduction band of TiO<sub>2</sub> and of the HOMO level for

electron acceptance from the I<sup>-</sup>/I<sub>3</sub><sup>-</sup> redox couple in the electrolyte, giving highly efficient electron transfer at the interfaces between TiO<sub>2</sub>/dye and dye/electrolyte, respectively; (3) anchoring group(s) reacting with the TiO<sub>2</sub> surface to promote unidirectional electron injection from the excited state of dye to the conduction band of TiO<sub>2</sub>; (4) intramolecular charge-transfer(CT)-type absorption to give vectorial electron transfer in dye molecules toward the TiO<sub>2</sub>; (5) chemical stability of the redox reactions to achieve long-term durability of DSC.

To obtain a panchromatic absorption band, the  $\pi$ -conjugated system of the sensitizing molecules should be expanded. Introduction of electron-donating and -withdrawing groups to dye structure gives CT character of absorption and wide and high absorptivity. According to these requirements and strategies in molecular design of photosensitizers, we designed and synthesized a series of oligoene dyes that have a carboxylic group as the anchoring group to TiO<sub>2</sub> and a cyano group (or carboxylic group) as the electron-accepting group and a dialkyl (or diphenyl) amino group as the electron-donating group (Scheme 1). Numbers of conjugating carbon-carbon double bonds and dialkyl (or diphenyl) amino groups were also considered in molecular design. During our investigation, similar and comparable polyene molecules were applied to DSC and the cell sensitized by the best polyene sensitizing dye was reported to give 6.8% of the conversion efficiency.<sup>29</sup>

In this paper, we report the photoelectrochemical properties of a series of designed dyes and IPCE and solar cell performance of DSCs based on these dyes. In femtosecond mid-IR transient absorption spectroscopic analysis, very fast electron injection from the excited state of these dyes molecules to the conduction band of TiO<sub>2</sub> was confirmed to occur as observed in the case of the ruthenium sensitizing complexes.

## Experiments

**Synthesis of Polyene Dyes.** A series of oligoene dyes were synthesized by condensation of the appropriate aldehyde and methyl cyanoacetate (diethyl malonate for **2c**). All reagents were commercially available and used without further purification. For example, **1a** was synthesized as follows. 4-Dimethylaminobenzaldehyde, methyl cyanoacetate, and piperidine were dissolved in ethanol and refluxed for 2 h. After the reaction, the precipitated ester was filtered and washed with ethanol. The ester was hydrolyzed in 5% KOH ethanol by refluxing for 2 h. The reaction mixture was diluted by water and the solution pH was adjusted to 6 by adding 10% HCl at r.t. The precipitate was then filtered and washed by ethanol. The precipitate was purified by column chromatography (hexane/ethyl acetate) and the recrystallization from ethanol solution gave pure **1a** as yellow powder.

**Instruments.** Absorption, excitation, and emission spectra in ethanolic solution were recorded on a spectrometer (Bunkoh-keiki, UV/vis/NIR spectrophotometer) and a spectrofluorometer (Bunkoh-keiki, FP-6600 spectrofluorometer) in different concentrations. Absorption spectra of the dyes adsorbed on TiO<sub>2</sub> films were recorded on a spectrometer (Shimadzu, UV-2101PC). Cyclic voltammetry was conducted in a distilled *N,N*-dimethylformamide (DMF) or an acetonitrile solution containing 1.0 mM ( $M = \text{mol}\cdot\text{dm}^{-3}$ ) of the dye and 0.1 M of tetrabutylammonium perchlorate as supporting electrolyte. Reference electrode, Ag/AgCl; working and counter electrode, Pt; scan rate, 100 mV·s<sup>-1</sup>; temperature, 15 °C.

(15) Sayama, K.; Hara, K.; Mori, N.; Satsuki, M.; Suga, S.; Tsukagoshi, S.; Abe, Y.; Sugihara, H.; Arakawa, H. *Chem. Commun.* **2000**, 1173.

(16) Sayama, K.; Tsukagoshi, S.; Hara, K.; Ohga, Y.; Shinpo, A.; Abe, Y.; Suga, S.; Arakawa, H. *J. Phys. Chem. B* **2002**, *106*, 1363.

(17) Hara, K.; Sayama, K.; Ohga, Y.; Shinpo, A.; Suga, S.; Arakawa, H. *Chem. Commun.* **2001**, 569.

(18) Hara, K.; Tachibana, Y.; Ohga, Y.; Shinpo, A.; Suga, S.; Sayama, K.; Sugihara, H.; Arakawa, H. *Sol. Energy Mater. Sol. Cells* **2003**, *77*, 89.

(19) Hara, K.; Sato, T.; Katoh, R.; Furube, A.; Ohga, Y.; Shinpo, A.; Suga, S.; Sayama, K.; Sugihara, H.; Arakawa, H. *J. Phys. Chem. B* **2003**, *107*, 597.

(20) Hara, K.; Kurashige, M.; Dan-oh, Y.; Kasada, C.; Shinpo, A.; Suga, S.; Sayama, K.; Arakawa, H. *New J. Chem.* **2003**, *27*, 783.

(21) Ehret, A.; Stuhl, L.; Spitler, T. *Electrochim. Acta* **2000**, *45*, 4553.

(22) Ehret, A.; Stuhl, L.; Spitler, T. *J. Phys. Chem. B* **2001**, *105*, 9960.

(23) Wang, Z.-S.; Li, F.-Y.; Huang, C.-H. *Chem. Commun.* **2000**, 2063.

(24) Wang, Z.-S.; Li, F.-Y.; Huang, C.-H.; Wang, L.; Wei, M.; Jin, L.-P.; Li, N.-Q. *J. Phys. Chem. B* **2000**, *104*, 9676.

(25) Wang, Z.-S.; Li, F.-Y.; Huang, C.-H.; Wang, L.; Wei, M.; Jin, L.-P.; Li, N.-Q. *J. Phys. Chem. B* **2001**, *105*, 9210.

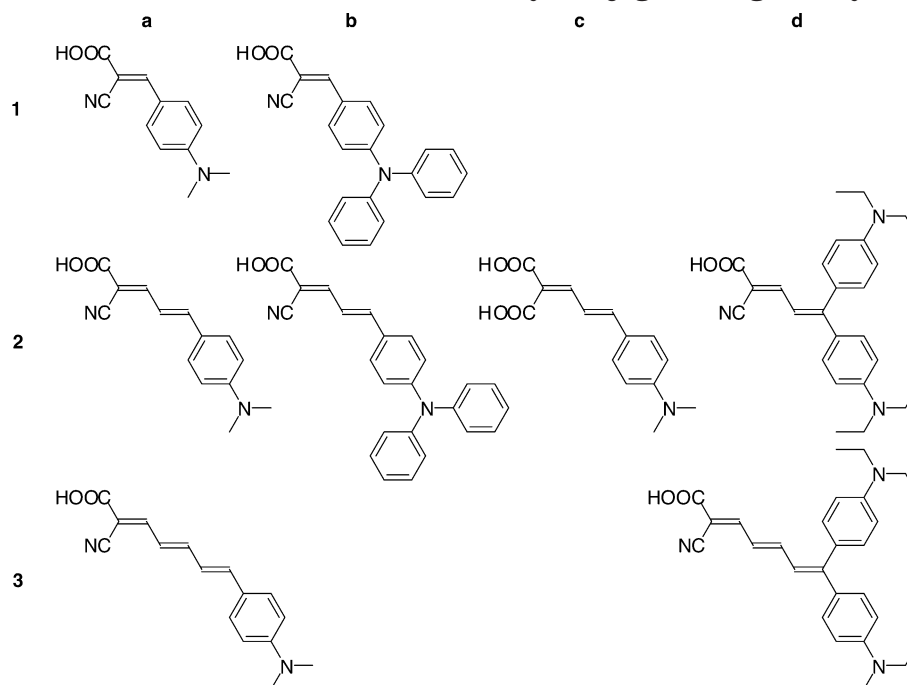
(26) Yao, Q.-H.; Shan, L.; Li, F.-Y.; Yin, D.-D.; Huang, C.-H. *New J. Chem.* **2003**, *27*, 1277.

(27) Yao, Q.-H.; Meng, F.-S.; Li, F.-Y.; Tian, H.; Huang, C.-H. *J. Mater. Chem.* **2003**, *13*, 1048.

(28) Meng, F.-S.; Yao, Q.-H.; Shen, J.-G.; Li, F.-Y.; Huang, C.-H.; Chen, K.-C.; Tian, H. *Synth. Met.* **2003**, *137*, 1543.

(29) Hara, K.; Kurashige, M.; Ito, S.; Shinpo, A.; Suga, S.; Sayama, K.; Arakawa, H. *Chem. Commun.* **2003**, 252.

## Scheme 1. Chemical Structure of Phenyl-Conjugated Oligoene Dyes



**Preparation of Dye-Adsorbed TiO<sub>2</sub> Films.** TiO<sub>2</sub> films for conventional spectroscopy and transient measurements were prepared by modifying the literature method<sup>30</sup> to give less scattering films on a sapphire plate that is transparent in the UV, vis, and IR region. A mixture of 37 mL of Ti(O<sup>i</sup>Pr)<sub>4</sub> and 10 mL of <sup>t</sup>PrOH was hydrolyzed by dropwise addition into an aqueous acetic acid (80 mL of glacial acetic acid in 250 mL of water) at 0 °C for 1 h under vigorous stirring to give a cloudy suspension. The suspension was kept standing at 80 °C for 4 h under vigorous stirring to give 200 mL of viscous sol, being allowed to cool to room temperature to give a gel. The resulting bluish white gel was autoclaved in a Teflon-lined stainless autoclave at 230 °C for 12 h. The supernatant solution was removed from the precipitate by decantation and the mixture of precipitate and a few drops of Triton-X was sonicated for 30 min in ultrasonic bath and then stirred by a magnetic stirrer for several days. The resulting paste was spread on a sapphire plate, which was washed by a piranha solution (H<sub>2</sub>SO<sub>4</sub>:H<sub>2</sub>O<sub>2</sub> = 4:1) beforehand, by the doctor blading technique using Scotch tape (Sumitomo 3M) as a spacer and sintered at 400 °C for 1 h. The thickness of the resulting films, measured by a profilometer (Sloan, Dectak3), was ca. 3 μm. For the fabrication of solar cells, we used two different types of mesoporous TiO<sub>2</sub> films. Film **a**: Double-layered TiO<sub>2</sub> films were prepared from commercially available TiO<sub>2</sub> sol based on nanosized particles (Solaronix, Ti-nanoxide T, average diameter: *d* = ca. 13 nm) and commercially available micrometer-sized particles (Catalysis & Chemicals Industry, HPW300C, *d* = ca. 300–400 nm). Ti-nanoxide T sol was spread on an optically transparent conducting fluorine-doped SnO<sub>2</sub> (FTO)-coated glass (Nippon Sheet Glass, 10 Ω/sq.) by doctor blading using Scotch tape as a spacer. After heating at 260 °C for 10 min, the second sol, which consisted of HPW300C and water, was spread on the top of the film by doctor blading. After sintering at 500 °C for 30 min, the thicknesses of the first and second layer of TiO<sub>2</sub> films were ca. 10 and 4 μm, respectively. Film **b**: Single-layered more opaque TiO<sub>2</sub> films were prepared from commercially available nanosized particles (Nippon Aerosil, P25). As reported, P25 was dispersed in an aqueous solution with acetylacetone and Triton X-100, and the paste was spread on a FTO-coated glass by doctor blading. After the paste was sintered at 450 °C for 30 min, mesoporous TiO<sub>2</sub> films

with ca. 10-μm thickness and 55% porosity were obtained. The films for the cells were treated with TiCl<sub>4</sub> before dye adsorption, where the sintered films were dipped in 0.05 M of aqueous TiCl<sub>4</sub> acidified by diluted hydrogen chloride (Wako, practical-grade) at 80 °C for 30 min and rinsed by water.

Dye molecules were adsorbed on TiO<sub>2</sub> films using 3 × 10<sup>-4</sup> M of ethanolic or acetonitrile solutions for spectroscopic analyses. For the solar cell measurements, the dye adsorption was conducted using an acetonitrile solution containing 5 × 10<sup>-4</sup> M of dye and 0.04 M of 3α,7α-dihydroxy-5β-cholic acid (chenodeoxycholic acid, Wako, guaranteed-grade) as a co-adsorbate. The dyed films were left standing in acetonitrile overnight to remove the physically adsorbed dye completely before measurements.

**Solar Cell Performance Measurements.** The sandwich-type two-electrode cell consists of dye-adsorbed TiO<sub>2</sub> film **a** or **b** as a working electrode and an ITO (Geomatecs, 10 Ω/sq.) glass with sequentially sputtered chromium (400 Å) and platinum (1000 Å) as a counter electrode. Two different electrolyte compositions were employed: Electrolyte **1**: 0.5 M of tetra-*n*-propylammonium iodide (Wako, guaranteed-grade) and 0.05 M of I<sub>2</sub> (Wako, reagent-grade) in ethylenecarbonate/acetonitrile = 6/4 mixed solution (Wako, guaranteed-grade); electrolyte **2**: 0.6 M of 1,2-dimethyl-3-propylimidazolium iodide (DMPImI, Shikoku Corp.), 0.1 M of LiI (Wako, guaranteed-grade), 0.1 M of I<sub>2</sub>, and 1 M of 4-*tert*-butylpyridine (tBP, Aldrich, 99%) in methoxyacetonitrile (Aldrich, 99+%). I<sub>2</sub> was purified by sublimation, and tBP, ethylenecarbonate, and acetonitrile were distilled before use. The other chemicals were used as delivered.

The action spectrum of IPCE was recorded on a commercial setup for IPCE measurement (Bunkoh-keiki, PV-25 DYE) under 5 mW·cm<sup>-2</sup> of monochromatic light irradiation. The solar cell performance was measured under irradiation of AM 1.5 (100 mW·cm<sup>-2</sup>) simulated solar light (Yamashita Denso, YSS-50A) on a PC-controlled voltage current/source meter (Advantest, R6246) at 25 °C. The solar simulator was adopted to the Japanese Industrial Standard for amorphous solar cells in the cell efficiency determination (JIS C 8933).

**Femtosecond Pump and Probe Transient Spectroscopy.** The detailed setup of a medium wavelength range infrared (mid-IR) femtosecond pump and probe spectrometer used for the time-resolved electron injection dynamics study has been described elsewhere.<sup>31</sup> The setup is based on an amplified 1-kHz femtosecond Ti/sapphire laser system and

(30) Zaban, A.; Ferrere, S.; Sprague, J.; Gregg, B. A. *J. Phys. Chem. B* **1997**, *101*, 55.

**Table 1. Photoelectrochemical Properties of Phenyl-Conjugated Oligoene Dyes<sup>a</sup>**

dye	$\lambda_{\max}$	$\epsilon_{\max}$	$\lambda_{\text{ex}}$	$\lambda_{\text{em}}$	$E_{0-0}$	$E_{\text{ox}}^{\text{p}}$	$E_{\text{red}}$
<b>1a</b>	378	37000	397	450	3.0	1.16	-1.8
<b>1b</b>	386	33800	417	550	2.8	1.21	-1.6
<b>2a</b>	412	30000	431	535	2.6	0.99	-1.6
<b>2a<sup>b</sup></b>	457	33500					-1.0 vs NHE
	(tBuOH/AN = 1:1)	(MeOH)					
<b>2b</b>	417	25000	417	548	2.6		
<b>2c</b>	416	13900	425	542	2.5	0.86	-1.6
<b>2d</b>	443	33700	529	557	2.3	0.99	-1.3
<b>3a</b>	434	30500	510	658	~2.1	0.80	-1.3
<b>3d</b>	470	41500	538	643	~2.0	0.75	-1.2

<sup>a</sup> Spectra were observed at  $1.6 \times 10^{-5}$  mol·dm<sup>-3</sup> in ethanol.  $\lambda_{\max}$ , absorption maximum wavelength;  $\epsilon_{\max}$ , absorption coefficient at  $\lambda_{\max}$ ;  $\lambda_{\text{ex}}$ , excitation maximum wavelength;  $\lambda_{\text{em}}$ , emission maximum wavelength;  $E_{0-0}$ , energy gap determined from the cross section of excitation and emission spectra;  $E_{\text{ox}}^{\text{p}}$ , peak potential of cathodic current vs Ag/AgCl in DMF;  $E_{\text{red}}$ , reduction potential vs Ag/AgCl in DMF calculated from  $E_{\text{ox}}^{\text{p}}$  and  $E_{0-0}$ ;  $\lambda_{\text{film}}$ , absorption maximum wavelength on TiO<sub>2</sub> film. <sup>b</sup> From ref 29.

nonlinear frequency-mixing techniques. Dye-adsorbed TiO<sub>2</sub> film on a sapphire plate whose optical density was higher than 3 was excited at 400 nm under atmospheric conditions. The transient mid-IR (1900–2050 cm<sup>-1</sup> = ca. 5  $\mu\text{m}$ ) signal from electrons injected to the conduction band of TiO<sub>2</sub> film from the photoexcited state of dye was probed. During the measurement, the sample film was scanned continuously to avoid permanent photodegradation of the dye.

## Results and Discussion

**Photoelectrochemical Properties of Phenyl-Conjugated Oligoene Dyes.** Photochemical properties of the oligoene dyes in ethanol and their electrochemical properties in DMF were summarized in Table 1. The reported data of **2a** were also listed for comparison.<sup>29</sup> Extension of methine unit (**1** to **3**) induced a bathochromic shift of the absorption spectrum due to the expansion of  $\pi$ -electron systems conjugated with a phenyl ring. Replacement of *N,N*-dimethylanilino unit (**a**) with triphenylamino unit (**b**) or introduction of another *N,N*-diethylanilino group (**d**) also induced a bathochromic shift of the maximum wavelength due to the increment of donation ability of the phenylamino part. Spectral shape was not changed by the replacement of a cyano group with carboxylic acid (**2a** to **2c**) but the absorption coefficient was decreased due to the increase of the molecular symmetry. Absorption, excitation, and emission spectra were very sensitive to the solvent as observed in the case of **2a** in ethanol and in tBuOH/AN = 1:1 solution.<sup>29</sup> The spectra also varied depending on concentrations as is shown in the case of **2a** ethanolic solution (Figure 1). Absorption spectra were recorded using a 1-mm optical path length cell by transmission setup, and emission spectra were recorded from the excited side of the cell. The absorption maximum wavelength was gradually shifted from 412 nm at  $1.6 \times 10^{-5}$  M to 453 nm at  $3.2 \times 10^{-4}$  M. The emission spectrum was more drastically changed. The maxima were observed around 530 nm at concentrations lower than  $3.2 \times 10^{-5}$  M, but the peak was suddenly shifted to 570 nm at higher concentration conditions. The emission intensity did not change linearly with increase of the concentration. On changing of the peak position,

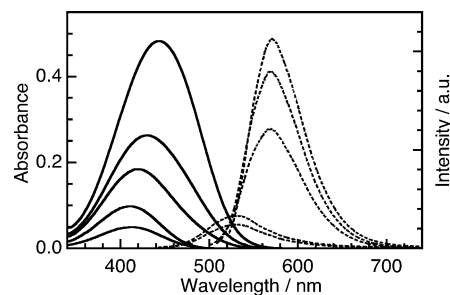
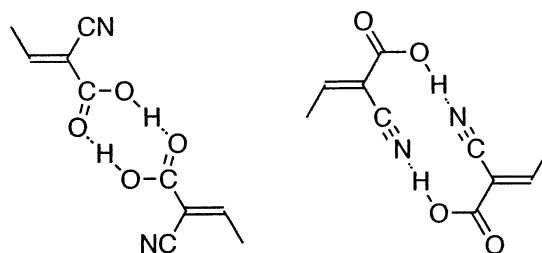


**Figure 1.** Absorption and emission spectra of **2a** in ethanolic solution: 1-mm optical path length cell,  $1.6 \times 10^{-5}$ ,  $3.2 \times 10^{-5}$ ,  $6.4 \times 10^{-5}$ ,  $1.07 \times 10^{-4}$ ,  $1.6 \times 10^{-4}$  M (from bottom to top).

### Scheme 2. Dimerized Structure of Phenyl-Conjugated Oligoene Dyes through the Hydrogen Bond of Carboxylic Acid Group and Cyano Group



the intensity was suddenly increased and leveled off at a higher concentration than  $6.4 \times 10^{-5}$  M. The changes with increase of concentration are probably explained as being due to the dimerization through the hydrogen bonds of the carboxylic groups (Scheme 2) or the formation of stacked aggregates through the planar conjugated molecular structure (**a** and **c**). The dimer structure in Scheme 2 could be rationalized by the IR spectra of oligoene dyes (see Supporting Information). The stretching vibrational band of C=O in carboxylic acid is shifted to a smaller wavenumber by dimerization through a hydrogen bond, and those of dimerized  $\alpha,\beta$ -unsaturated and aryl carboxylic acid appear at 1710–1680 cm<sup>-1</sup>. While C=O of **2c** appearing at 1692 cm<sup>-1</sup> is in the normal region, those of **1a**, **2a**, and **2d** were observed at much smaller wavenumbers of 1662, 1673, and 1663 cm<sup>-1</sup>, respectively. Both **3a** and **3d** only show two quite weak and very broad bands around 1700 and 1660 cm<sup>-1</sup>, which might be described as the presence of monomer and dimer in solid. These observations mean that they could form tightly hydrogen-bonded dimers through both two carbonyls and carbonyl and cyano groups. Weakening of not only broad O–H but also C≡N stretching bands supports the formation of hydrogen bonding through CN···HOC. **1b** and **2b**, however, show the peak at 1686 and 1706 cm<sup>-1</sup>, respectively, and a relatively stronger O–H stretching band. A sterically hindered triphenylamine unit might prevent the formation of a hydrogen-bonded dimer in crystal packing.

Cyclic voltammograms of all oligoene dyes showed irreversible waves both for cathodic and anodic scans. Table 1 lists the oxidation peak potentials of cathodic currents and the reduction potential calculated from the oxidation potential and the energy of the cross section of excitation and emission spectra observed in low-concentration conditions. According to the expansion of the  $\pi$ -conjugation system of the phenyl-conjugated oli-

(31) Asbury, J. B.; Ellingson, R. J.; Ghosh, H. N.; Ferrere, S.; Nozik, A. J.; Lian, T. *J. Phys. Chem. B* **1999**, *103*, 3110.

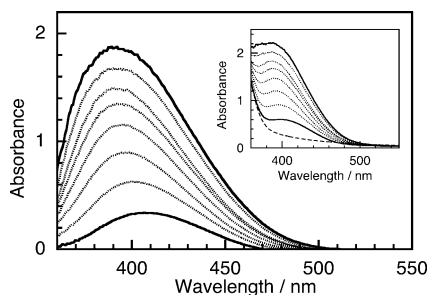


**Figure 2.** Absorption spectral change of **3a** on mesoporous TiO<sub>2</sub> film: 10, 20, 30, 40, 50, 60, 90, and 120 s after immersion of mesoporous TiO<sub>2</sub> film in  $3 \times 10^{-4}$  M acetonitrile solution of **3a**. Insert: the observed absorption spectra of **3a** when adsorbed on TiO<sub>2</sub> film: (---) absorption spectrum of bare TiO<sub>2</sub> film.

gone dyes, the oxidation potential of the ground state (HOMO level) was shifted to negative, and the reduction potential (LUMO level) was shifted to positive. Increase of donor ability of the amino unit caused positive shift of both HOMO and LUMO levels, and the shift of the LUMO level was found to be larger than that of HOMO. The LUMO levels of these dyes were negative enough to inject electrons into the conduction band of TiO<sub>2</sub> ( $-0.52$  V vs SCE in H<sub>2</sub>O at pH = 2<sup>32</sup>), and the HOMO levels were positive enough when iodide ion is employed as an electron donor in electrolyte ( $0.24$  V vs SCE<sup>33</sup>) of DSC systems.

**Dye Adsorption Behavior on TiO<sub>2</sub>.** The dyes can adsorb on TiO<sub>2</sub> from the variety of solutions because of the presence of a carboxylic group in the molecules. Dye adsorption was completed within a few to tens of minutes from acetonitrile solution, and within a few hours from ethanolic solution. Figure 2 shows the time-course change of the absorption spectrum of **3a** that is adsorbed on TiO<sub>2</sub> film during soaking in the acetonitrile solution, where the absorption due to TiO<sub>2</sub> film was subtracted (see insert). The absorption peak of **3a** in acetonitrile was 416 nm, but the maximum of **3a** on TiO<sub>2</sub> film was obviously shifted to a shorter wavelength and the degree of the shift was increased with increasing the amount of the dye on TiO<sub>2</sub> film. The spectral change was quite in contrast to the change in solution since the peak was located at <400 nm after the adsorption was saturated. The blue shift of the absorption peak on TiO<sub>2</sub> was also observed in **1a**, **1b**, **2a**, and **2b** and the degrees of the shifts were ca. 20 nm, and **2c** with two carboxylic groups showed slight red shift of the absorption. These results suggest that the adsorption on TiO<sub>2</sub> through the carboxylic group leads to the formation of aggregates that are different from those in solution. The conjugated planar structures of **1a**, **1b**, **2a**, **2b**, and **3a** should be largely affected by the different aggregation on TiO<sub>2</sub>. Because it is possible that these stacked aggregation on TiO<sub>2</sub> may decrease electron injection due to intermolecular energy transfer, the dye adsorption for cell assembly was conducted by co-adsorption of dye molecules with chenodeoxycholic acid.<sup>4,5,19,20,34</sup>

**Solar Cell Performance.** The action spectrum of incident photon-to-current conversion efficiency (IPCE)

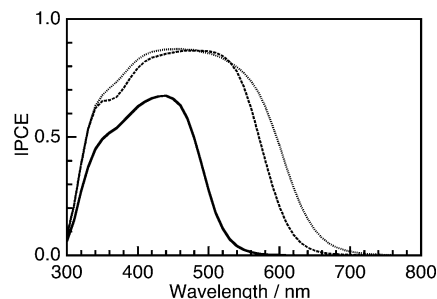


**Figure 3.** Action spectrum of incident photon-to-current conversion efficiency (IPCE) of oligoene dye-sensitized DSC: **1a** (—), **2a** (---), and **2c** (···).

of DSC represents the spectral dependence of the quantum yield of the current generation of the dye in the DSC system. IPCE spectra for **1a**, **2a**, and **2b** were shown in Figure 3. The observed IPCE values reflected the absorption spectra of the dye molecules adsorbed on TiO<sub>2</sub> films because the onset wavelength was shifted to longer wavelength by increasing the  $\pi$ -conjugated system of the dyes. The onsets of IPCE of DSC based on **3a** and **3d** dye reached 750 nm (data not shown). Interestingly, very high IPCE values were observed in the spectral range between 400 and 600 nm and the maximum values reached 80% for the examined dyes. These results strongly suggest that the absorbed photon-to-current conversion efficiency for phenyl-conjugated oligoene solar cells were quite high and close to unity in the range between 400 and 600 nm. Lower IPCE for **1a** could be due to the shortage of the amount of dye on TiO<sub>2</sub>, but not to the energy migration in aggregated dye, because **1a** showed comparable electron injection dynamics to the other dyes as discussed later.

Hara et al. reported the relationship between the LUMO level of the coumarin dyes and maximum IPCE values, pointing out that an energy gap more than 0.2 eV between the LUMO level of the dye and the conduction band edge of TiO<sub>2</sub> was necessary to obtain high IPCE value.<sup>19</sup> The present oligoene dyes have highly negative LUMO levels (Table 1), satisfying this energy gap rule, that is, highly efficient electron injection ability of the designed organic dye molecules.

Solar cell characteristics using several phenyl-conjugated oligoene dyes under irradiance of simulated AM 1.5 ( $100 \text{ mW}\cdot\text{cm}^{-2}$ ) were summarized in Table 2. As references, the values of DSCs sensitized by N719 dye {bis(tetrabutylammonium) salt of *cis*-dithiocyanato bis-(4,4'-dicarboxy-2,2'-bipyridine)ruthenium(II)} using the same TiO<sub>2</sub> films and electrolytes were also listed. The short-circuit photocurrent density ( $J_{sc}$ ) was increased by the expansion of the  $\pi$ -conjugated system of the dye. The observed  $J_{sc}$  under AM 1.5 irradiation coincided with the estimated values from the integration of the product of the photon flux of AM 1.5 spectrum and the IPCE value for each wavelength. Thus,  $J_{sc}$  was proportional to the absorption spectral range of the dye on TiO<sub>2</sub> film. The open-circuit photovoltage ( $V_{oc}$ ) of the cells based on **1a**, **b** and **2a–d** was comparable to or higher than those of the cells based on N719. Generally,  $V_{oc}$  was determined by the potential difference between the Fermi level of TiO<sub>2</sub> under irradiation and redox potential of I<sup>-</sup>/I<sub>3</sub><sup>-</sup> couple and seems to be independent of the redox potentials of sensitizing dyes. While reported  $V_{oc}$

(32) Hagfeldt, A.; Grätzel, M. *Chem. Rev.* **1995**, *95*, 49.

(33) Sauv e, G.; Cass, M. E.; Coia, G.; Doig, S. J.; Lauer mann, I.; Pomykal, K. E.; Lewis, N. S. *J. Phys. Chem. B* **2000**, *104*, 6821.

**Table 2. Solar Cell Performance of Phenyl-Conjugated Oligoene Dye-Sensitized Solar Cells<sup>a</sup>**

dye	TiO <sub>2</sub> film	electrolyte	area (cm <sup>2</sup> )	J <sub>sc</sub> (mA·cm <sup>-2</sup> )	V <sub>oc</sub> (V)	fill factor	η (%)
1a	a	1	0.409	4.3	0.79	0.65	2.2
1a	b	1	0.27	5.6	0.72	0.61	2.4
1a <sup>c</sup>	b	1	0.216	5.5	0.67	0.62	2.3
1b	a	1	0.395	6.3	0.77	0.67	3.3
1b	b	1	0.14	7.2	0.67	0.63	3.0
1b <sup>c</sup>	b	1	0.184	6.9	0.64	0.57	2.5
2a	a	1	0.486	8.7	0.73	0.72	4.7
2a	b	1	0.16	9.9	0.70	0.57	4.0
2a <sup>c</sup>	b	1	0.184	7.9	0.66	0.58	3.1
2a <sup>b</sup>	c	3	0.245	10.4	0.71	0.74	5.5
2b	a	1	0.403	11.1	0.73	0.66	5.3
2b	b	1	0.14	11.5	0.71	0.62	5.1
2b <sup>c</sup>	b	1	0.180	9.7	0.74	0.62	4.5
2c	a	1	0.21	10.7	0.69	0.55	4.1
2c <sup>c</sup>	b	1	0.184	9.1	0.66	0.58	3.1
2d	a	1	0.15	10.9	0.65	0.53	3.8
3a	a	1	0.17	10.4	0.62	0.56	3.6
3a <sup>c</sup>	b	1	0.179	9.2	0.58	0.56	3.0
3d	a	1	0.20	16.4	0.61	0.66	6.6
3d	b	1	0.15	11.9	0.62	0.62	4.6
3d <sup>c</sup>	b	1	0.179	11.3	0.61	0.62	4.3
N719 <sup>c</sup>	a	1	0.426	15.7	0.74	0.67	7.7
N719 <sup>c</sup>	b	2	0.21	15.1	0.68	0.58	6.0

<sup>a</sup> The solar cell performance was measured under irradiation of AM 1.5 simulated solar light at 25 °C. Film a: Double-layered TiO<sub>2</sub> film prepared from Ti-nanoxide T and HPW300C. Film b: Single-layered TiO<sub>2</sub> film prepared from P25. Film c: Opaque TiO<sub>2</sub> film prepared from nanoparticles and large particles by screen printing.<sup>29</sup> Electrolyte 1: 0.5 M of tetra-*n*-propylammonium iodide and 0.05 M of I<sub>2</sub> in ethylenecarbonate/acetonitrile = 6/4. Electrolyte 2: 0.6 M DMPImI, 0.1 M LiI, 0.1 M I<sub>2</sub>, and 1 M of tBP in methoxyacetonitrile. Electrolyte 3: 0.6 M DMPImI, 0.1 M LiI, 0.05 M I<sub>2</sub>, and 0.56 M of tBP in acetonitrile.<sup>29</sup> <sup>b</sup> From ref 29. <sup>c</sup> Without chenodeoxycholic acid.

values for DSC based on organic dyes were generally lower than those obtained in the cells based on ruthenium complexes, the present dye-sensitized solar cells showed large V<sub>oc</sub>. The change of V<sub>oc</sub> could be the result of the potential shift of the Fermi level of TiO<sub>2</sub> because the redox potential of I<sup>-</sup>/I<sub>3</sub><sup>-</sup> is not varied so much as long as the same electrolyte is used. A possible explanation for this tendency could be the basic property of the dye molecules with amino group that affect the Fermi level of TiO<sub>2</sub>. Co-adsorption of chenodeoxycholic acid with dye on the surface of TiO<sub>2</sub> improved each of J<sub>sc</sub>, V<sub>oc</sub>, and fill factor and enhanced conversion efficiency of the cell.<sup>4,5,19,20,34</sup> The highest photon-to-electricity conversion efficiency was obtained when 3d was employed as an organic sensitized with chenodeoxycholic acid and Ti-nanoxide T TiO<sub>2</sub> film. The respectable efficiency can be rationalized as being due to suppression of recombination of the injected electron at the interfaces between TiO<sub>2</sub> and the electrolyte.

**Femtosecond Pump and Probe Transient Spectroscopy.** Recently, the dynamics of photoinduced electron injection from the excited state of dyes to the conduction band of TiO<sub>2</sub> have been studied using femtosecond pump and probe transient absorption spectroscopy.<sup>34–37</sup> Conduction band electrons and valence band

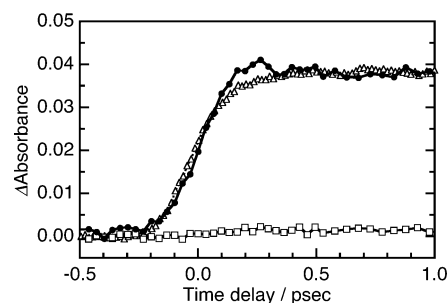


**Figure 4.** Transient mid-IR absorption for probing the injected electron signal at 2000 cm<sup>-1</sup> after femtosecond 400-nm excitation: (●) 1a dye-adsorbed mesoporous TiO<sub>2</sub> film and (□) naked TiO<sub>2</sub> film as references, and intensity normalized response of (Δ) silicon wafer.

holes in semiconductors have strong absorption in the mid-IR region that consist of free carrier absorptions which are often broad and increase with wavelength, absorption of trap states, and intraband transitions between different sub-bands in the conduction and valence bands. Thus, the transient mid-IR absorption spectroscopy can provide direct evidence of electron injection by dye sensitization.<sup>31,38,39</sup>

Figure 4 shows the transient absorption change for 1a on TiO<sub>2</sub> film observed in the mid-IR region (around 2000 cm<sup>-1</sup>) following excitation at 400 nm. A negligible transient signal for naked TiO<sub>2</sub> was observed under identical conditions. The rise of the transient signal was quite fast and the response was comparable to the signal observed for silicon wafer, corresponding to the instrumental time resolution. In contrast to the case of N3 dye on TiO<sub>2</sub>,<sup>39</sup> no slower injection component was observed in the case of 1a. Figure 5 shows the intensity-normalized transient signals observed for all phenyl-conjugated oligoene dyes on TiO<sub>2</sub> in different time windows. The decay within 1 ns is expected to be mainly due to the decrease of absorption cross section of electron in conduction band by relaxation from higher states to conduction band edge or by trapping, rather than due to back-electron transfer to the oxidized dye.<sup>37,40</sup> Very fast (<100 fs) and single-component electron injection to TiO<sub>2</sub> was observed for all examined dyes. Most of the signals in all time windows were almost identical within the experimental error limits. These results demonstrate that all phenyl-conjugated oligoene dyes examined here can inject electrons very efficiently within a very short time from their excited states to the conduction band of TiO<sub>2</sub>; thus, the quantum yields of electron injection are expected to be close to unity. These observations coincide well with the IPCE measurements and reveal the high performance of oligoene dyes as sensitizers for DSC.

## Conclusions

A series of novel phenyl-conjugated oligoene dyes with cyano groups or carboxylic groups as the electron

(34) He, J.; Benkő, G.; Korodi, F.; Polivka, T.; Lomoth, R.; Åkermark, B.; Sun, L.; Hagfeldt, A.; Sundström, V. *J. Am. Chem. Soc.* **2002**, *124*, 4922.

(35) Tachibana, Y.; Moser, J. E.; Grätzel, M.; Klug, D. R.; Durrant, J. R. *J. Phys. Chem.* **1996**, *100*, 20056.

(36) Hannappel, T.; Burfeindt, B.; Storck, W.; Willig, F. *J. Phys. Chem. B* **1997**, *101*, 6799.

(37) Benko, G.; Kallioinen, J.; Korppi-Tommola, J. E. I.; Yartsev, A. P.; Sundström, V. *J. Am. Chem. Soc.* **2002**, *124*, 489.

(38) Ellingson, R. J.; Asbury, J. B.; Ferrere, S.; Ghosh, H. N.; Sprague, J. R.; Lian, T.; Nozik, A. J. *J. Phys. Chem. B* **1998**, *102*, 6455.

(39) Asbury, J. B.; Hao, E.; Wang, Y.; Ghosh, H. N.; Lian, T. *J. Phys. Chem. B* **2001**, *105*, 4545.

(40) Asbury, J. B.; Anderson, N. A.; Hao, E.; Ai X.; Lian, T. *J. Phys. Chem. B* **2003**, *107*, 7376.

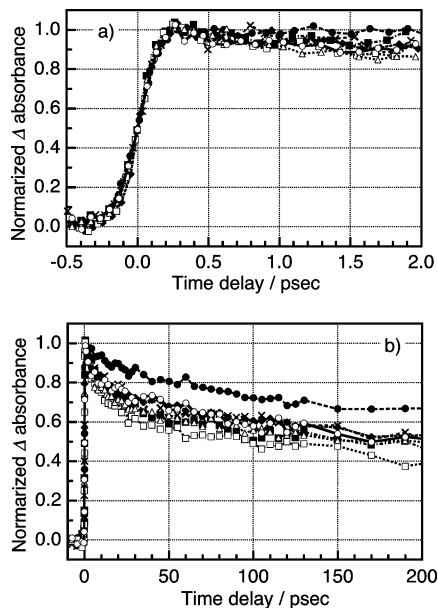


**Figure 5.** Intensity normalized transient mid-IR absorption for dye-adsorbed mesoporous  $\text{TiO}_2$  films probing the injected electron signal at  $2000\text{ cm}^{-1}$  after femtosecond 400-nm excitation in different time windows: (a)  $-0.5$  to  $2.0$  and (b)  $-10$  to  $200$  ps; (●) **1a**, (○) **1b**, (▲) **2a**, (△) **2b**, (◇) **2c**, (×) **2d**, (■) **3a**, and (□) **3b**.

acceptor units and disubstituted amino groups as the electron donor units were synthesized. Absorption spectrum and redox potentials were found to be controllable by expansion of the  $\pi$ -conjugated length, and a number of disubstituted amino groups. Dye-sensitized solar cells based on the phenyl-conjugated oligoene dyes showed respectable photovoltaic performances under 1 sun

irradiation conditions. From the IPCE spectra and the photocurrent densities, absorbed photon-to-current conversion efficiencies of the cells were almost unity. Transient absorption spectroscopy in the mid-IR region revealed very fast electron injection from the excited states of the dyes to the conduction band of  $\text{TiO}_2$ . Strategies of molecular design discussed in the present paper could be an important guideline for organic dye-sensitized solar cells.

**Acknowledgment.** This work was partially supported by a Grant-in-Aid for the Creation of Innovations through Business-Academic-Public Sector Cooperation, Open Competition for the Development of Innovative Technology (No. 12310) from the Ministry of Education, Culture, Sports, Science and Technology of Japan, by International Joint Research Grant Program (No. 2002RB048) from the New Energy and Industrial Technology Development Organization (NEDO), and by the Strategic Research Base, Frontier Research Center, (Graduate School of Engineering) Osaka University, from the Japan Government's Special Coordination Fund for Promoting Science and Technology. T.K. acknowledges the financial support by the Research Institute of Innovative Technology for the Earth (RITE), Japan. T.L. thanks the U.S. Department of Energy and the Petroleum Research Fund. T.L. is an Alfred P. Sloan fellow.

**Supporting Information Available:** Synthetic procedure and  $^1\text{H}$  NMR, IR, and mass spectral data for all oligoene dyes. This material is available free of charge via the Internet at <http://pubs.acs.org>.

CM0349708